EasyChair Preprint

№ 15429

Efficient Failure Information Propagation Under Complex Stress States in Fiber Reinforced Polymers: from Micro- to Meso-Scale Using Machine Learning

Johannes Gerritzen, Andreas Hornig and Maik Gude

December 4, 2024

Efficient Failure Information Propagation under Complex Stress States in Fiber Reinforced Polymers: From Micro- to Meso-scale using Machine Learning

Johannes Gerritzen[1,a*], Andreas Hornig[1,2,3,b] and Maik Gude[1,c]

[1] Institute of Lightweight Engineering and Polymer Technology,
TUD Dresden University of Technology, Holbeinstr. 3, 01307 Dresden, Germany

[2] Center for Scalable Data Analytics and Artificial Intelligence (ScaDS.AI) Dresden/Leipzig,
TUD Dresden University of Technology, Chemnitzer Straße 46b, 01187, Dresden, Germany

[3] Department of Engineering Science, Solid Mechanics and Materials Engineering,
University of Oxford, OX1 3PJ, Oxford, United Kingdom

[a]johannes.gerritzen@tu-dresden.de, [b]andreas.hornig@tu-dresden.de, [c]maik.gude@tu-dresden.de

* Corresponding author

Keywords: Fiber reinforced plastic, Machine Learning, Failure

Abstract The failure behavior of fiber reinforced polymers (FRP) is strongly influenced by their microstructure, i.e. fiber arrangement or local fiber volume content. However, this information cannot be directly used for structural analyses, since it requires a discretization on micrometer level. Therefore, current failure theories do not directly account for such effects, but describe the behavior averaged over an entire specimen. This foundation in experimentally accessible loading conditions leads to purely theory based extension to more complex stress states without direct validation possibilities. This work aims at leveraging micro-scale simulations to obtain failure information under arbitrary loading conditions. The results are propagated to the meso-scale, enabling efficient structural analyses, by means of machine learning (ML). It is shown that the ML model is capable of correctly assessing previously unseen stress states and therefore poses an efficient tool of exploiting information from the micro-scale in larger simulations.

Introduction

Fiber reinforced polymers (FRP) play a crucial role in lightweight applications due to their excellent specific properties [1]. This allows significant weight reduction and thus improvement of energy efficiency in the mobility sector and of frequently accelerated parts in general [2]. However, one major obstacle for the wider application of FRP is the challenge of joining FRP with dissimilar materials [3]. So far, adhesive bonding has been the widest spread solution [4]. This however is undesirable when considering end of life and recycling, because dejoining is impossible or requires a significant amount of effort. Hence, material preserving recycling has yet to be widely adopted for FRP [5].

One possible solution to improve the dejoinability, and thus the recyclability, of FRP is the implementation of mechanical joining technologies. However, these lead to significant changes in the local material structure and therefore the joints load bearing behavior [6]. Established failure criteria for FRP originate in thin walled materials with almost plane stress conditions [7]. Even though many theories have been extended to consider all stress components, even biaxial stress states still pose a significant challenge [8]. One significant contributing factor are the microscopic inhomogeneities of FRP, which strongly influence the failure behavior [9].

With rising computing power, the study of failure behavior by finite element analyses (FEA) on micro-scale has received more attention in research. The effect of fiber distribution as well as yarn alignment and waviness on elastic properties of entire plies has been studied with a special focus on draping effects in [10]. Pulungan et al. investigated the effect of local microstructure and RVE size on the failure behavior under transverse tension [11].

Such micro-scale models allow deep insight into the local behavior. However, their computational cost remains prohibitive for real world structures [12]. For elastic properties, homogenization approaches are well established to efficiently take information from the micro-scale into account on the meso-scale. This is enabled by the well accepted models on meso-scale. Given the lack thereof for FRP specific failure criteria under arbitrary stress states, the homogenization approach cannot directly be applied to failure behavior.

Fueled by the growing application of machine learning (ML) techniques, some approaches have been presented, obtaining data from micro-scale simulations and training various ML models on these data. Chen et al. used an RVE subjected to three stress components to predict critical loading conditions and trained these into an NN with all used data points being close to the failure envelope [13]. Wan et al. added the aspect of failure probability by analyzing multiple RVEs and taking all their results into account for the subsequent training [14]. None of these approaches take the simultaneous superposition of all stress components into account. Since this is crucial to accurately describe FRP behavior in the zone of a mechanical joint, the aim of this work is to establish a dataset from simulations on micro-scale representative volume elements (RVEs) under arbitrary loading conditions and subsequently train an ML model to assess criticality of a full stress state. This ML model is intended as alternative to established failure criteria, which can be incorporated into meso-scale FEA in future works.

Modeling approach

Material structure. Data regarding constituent behavior and uniaxial strengths are taken from the glass fiber-epoxy with Silenka E-Glass fibers and MY750/HY917/DY063 epoxy resin [15]. Here, data for a thermoset are used because of the amount of reliable data on its failure behavior and its status as the de facto standard for modeling FRP failure behavior. The different matrix system does not affect the presented development of a methodology for data driven failure determination and its propagation across length scales.

Based on the published data, constitutive models for the constituents are chosen. The glass fibers are modeled using an isotropic linear elastic model, with Young’s modulus and Poisson ratio taken directly from [15]. Failure is modeled as element deletion by a minimum/maximum principal strain criterion with corresponding strain values taken as uniaxial ones. For the epoxy resin, inelasticities have to be considered. These are modeled as purely plastic up to triaxiality dependent damage initiation, using LS-DYNA keywords *MAT_PIECEWISE_LINEAR_PLASTICITY and *MAT_ADD_DAMAGE_GISSMO as commonly described in literature, i.e. [16]. Under uniaxial tension and compression, this leads to excellent agreement with the published strength and failure strain: Under tension a maximum stress of 79 MPa occurs in the simulation and 80 MPa are given in the paper, with a corresponding failure strain of 4.9 % and 5 % respectively. Under compression, the constitutive model leads to a strength of 117 MPa, the paper states 120 MPa.

The constituents are assembled in a representative volume element (RVE) as shown in Fig. 1. Given the structured placement of individual fibers, identical edge lengths in x and y direction are highly important to ensure transversal isotropy in the RVE’s failure behavior. For this study, no fiber-matrix debonding is considered.

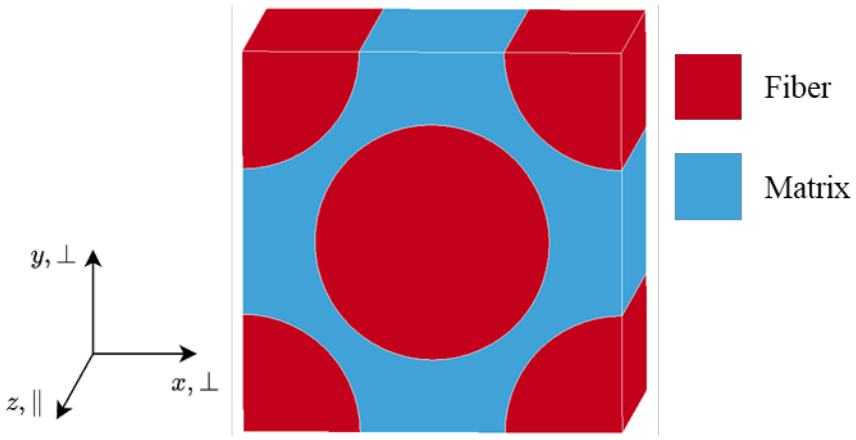

Figure 1 Geometrical arrangement of fibers in the RVE

Data generation. As database for subsequent ML model training a total of 5000 loadcases triggering all six stress components in the RVE are analyzed. To define these, 5000 unit vectors $\vec{v}$ in six dimensional stress space are taken such that the minimum distance of their endpoints is maximized, using the implementation of the maximin algorithm [17] in the open source Python package diversipy [18]. This ensures a good sampling of the full dimensional design space [19] and therefore yields ample information on the failure surface. An estimate for failure along each of the unit vectors is obtained by calculating the reserve factor f_{res} through the failure criterion proposed in [20] with the further adaptions from [21]; the best performing criteria on general stress states tested in [7]. Given the homogeneous formulation of the failure criterion, the estimates can be obtained from $\sigma_{\mathrm{fail}} \approx \vec{v} \,/\, f_{\mathrm{res}}$. To ensure simulations leading to failure, a termination time is chosen that is expected to lead to $2\sigma_{\mathrm{fail}}$ when extrapolating from the initial RVE stiffness. For the analysis, periodic boundary conditions are applied to the RVE using the *INCLUDE_UNITCELL keyword with 3 additional nodes as control points. To apply the intended stress states to the RVE, they are first transformed to their respective strain equivalent using the RVEs mesoscopic compliance matrix and from that to nodal displacements taking the RVE geometry into account. For details of the latter transformation, the reader is referred to [22]. The resulting values are applied as displacement boundary conditions to the control points.

Simulations are carried out on the high performance computing cluster Barnard at the NHR Center of TU Dresden. Given that the objective of this study is the modeling of the onset of failure, simulations are terminated once one element has been deleted. To reduce the data's dependency on integration step width, simulations are restarted from the last state before failure with the step size decreased and sampling frequency increased by a factor of 100.

From the simulation results, homogenized stress as well as failure information on the RVE are extracted, aligned by the simulation time, using the open source Python library lasso-python [23]. Here, information on failure mode is determined by the first material to fail, allowing for the differentiation between fiber failure (FF) and inter fiber failure (IFF). While neither failure model is triggered, a proxy mode "no failure" (nF) is added. This data is aggregated across all loadcases and loaded into three distinct databases with a unique identifier (UID) per loadcase.

For the training of the ML model, the database is split into training, test and validation sets, enforcing stratification by the loadcase UID to prevent cross contamination of the datasets. A ratio of 70:20:10 is chosen for this.

Machine learning. In this study, failure detection is treated as classification task. This is addressed by a fully connected neural network (NN), taking the six independent stress components as input vector in the form $[\sigma_1, \sigma_2, \sigma_3, \tau_{12}, \tau_{23}, \tau_{13}]$ and mapping them to the considered failure

modes. To achieve the highly non-linear mapping necessary, three hidden layers with 58, 65, 21 neurons respectively are used. The parameters were obtained by hyperparameter optimization, using the tool OmniOpt [24]. During this, the number of neurons per layer, batch size and learning rate were modified by the underlying Bayesian optimization algorithm until no improvement on the test loss occurred for 25 sequential iterations. For the output layer, the softmax activation function is used, leading to a probability prediction for the failure modes; all other layers have "Swish" [25] as activation function. The training is conducted using the Adam optimizer [26] for up to 200 epochs with categorical crossentropy loss, a batch size of 221 and a learning rate of 10^-2.033. Early stopping is activated to avoid overfitting if no improvement of the loss, evaluated on the test set, occurs for 50 epochs.

Results and discussion

Simulation. The RVE setup is first used to simulate uniaxial stress states. Strengths obtained from the simulations are given alongside experimental values in Table 1. From the comparison of the values, it becomes clear that the chosen setup is capturing the FRP's uniaxial failure behavior well in all cases except for transverse tension. This deviation can be attributed to the idealized fiber-matrix interface, since failure under transverse tension is typically initiated by fiber matrix debonding [27]. Therefore, results obtained by the presented RVE with the constitutive models for its constituents are considered representative for FRP and constitute a valid basis for developing a methodology for a data driven failure criterion.

Table 1 Strength values from experiment and RVE simulation

	$R_{\parallel}^{+}$ [MPa]	$R_{\parallel}^{-}$ [MPa]	$R_{\perp}^{+}$ [MPa]	$R_{\perp}^{-}$ [MPa]	$R_{\perp\parallel}$ [MPa]
WWFE [15]	1280	800	40	145	73
RVE	1292	799	77	139	67

From the 5000 loadcases, 4577 lead to IFF and 94 to FF. The remaining 329 cases did not yield usable results, 209 due to numerical problems and 120 since termination time was reached in the simulation before the RVE failed. To alleviate the substantial imbalance of the failure modes, an additional 100 loadcases with $\sigma_{\parallel} > 0.9\, R_{\parallel}^{+}$ or $\sigma_{\parallel} < -0.9\, R_{\parallel}^{-}$ were simulated, all leading to FF.

Machine Learning. During the training, of the ML model, loss and accuracy improve quickly for 35 epochs. Afterwards, model performance plateaus before signs of overfitting occur after 57 epochs. This is caught by the early stopping algorithm and training is terminated after 107 epochs with restoration to the state after 57 epochs. The development is shown in Fig. 2, with the loss on the left and accuracy on the right. The final model achieves an accuracy of 87 % on the training data and 84 % both on test and validation data.

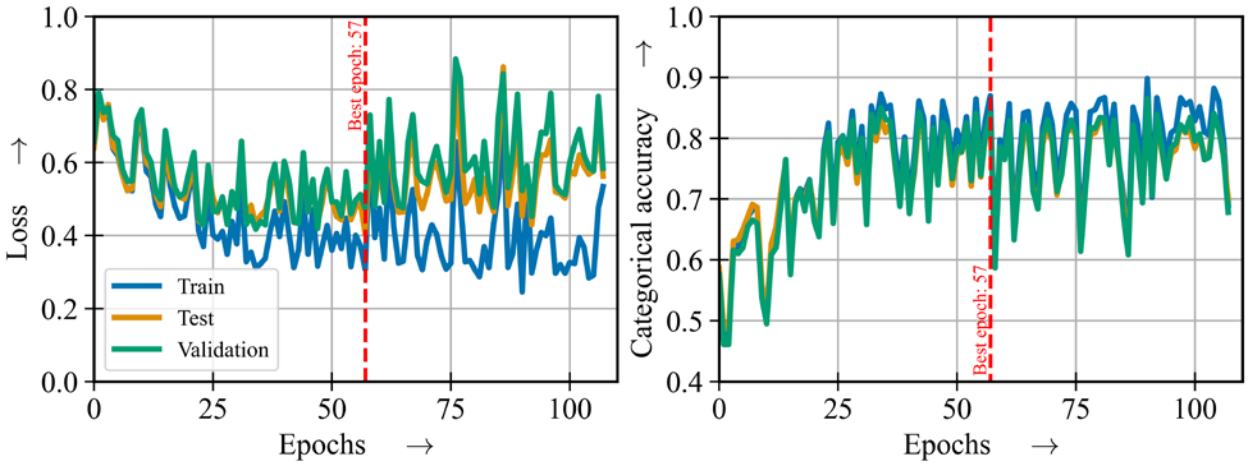

Figure 2 Development of performance metrics throughout model training

Additional insight into model performance is given confusion matrices. In this, each row represents the actual label and each column the model predictions. In each cell, the ratio of predictions for the respective true class is given. Hence, on the main diagonal represents correctly classified datapoints for each failure mode. On the left of Fig. 3, the confusion matrix for the validation dataset is shown. From this it becomes clear, that detecting IFF poses the highest challenge to the model, especially differentiating from nF. Similarly, a confusion of nF and IFF occurs, though significantly less frequently. This challenge can be attributed to the very high sampling frequency in the simulation when approaching the failure point. Therefore, the ternary decision has to be changed completely based on miniscule changes in the stress state.

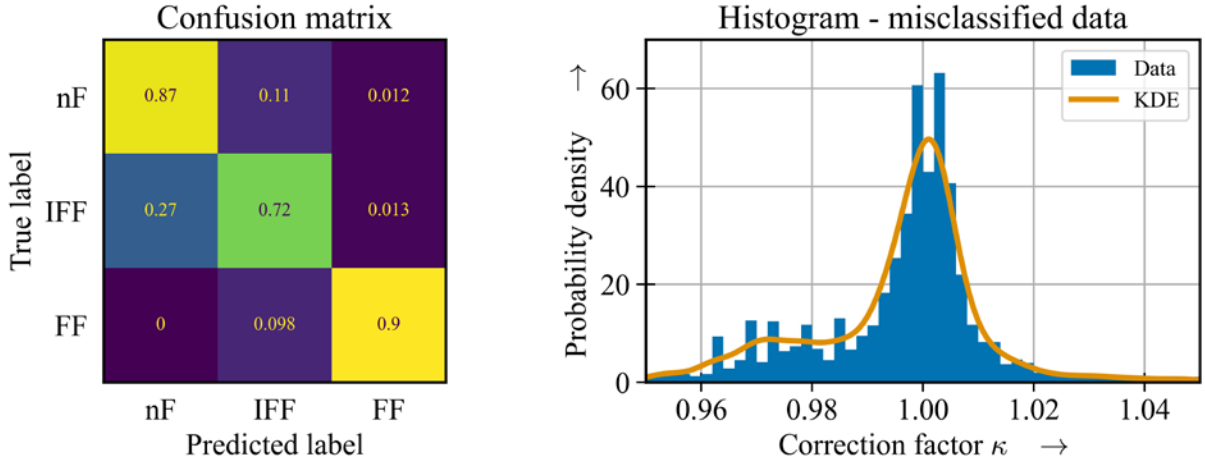

Figure 3 Confusion matrix for the validation data set (left) and correction factor κ for stress state necessary to obtain correct failure mode (right)

To quantify how far off the model predictions are in cases of misclassification, the stress state of misclassified data points is multiplied with a correction factor κ, which is smaller than 1 in cases where failure was predicted for uncritical stress states and greater than 1 otherwise. On the right in Fig. 3, a histogram of κ in the range 0.95 to 1.05 is shown alongside a kernel density estimate (KDE). Based on the KDE, an estimation of the increase in accuracy with percentage of acceptable deviation is possible. 77 % of misclassifications can be corrected κ in ±5 %, leading to an increase in accuracy of 12.3 %. With κ in ±1 %, still 49 % correction rate can be achieved, improving the accuracy by 8 %. This allows to take additional engineering judgement into account

Conclusion

A methodology for the development of a data driven failure criterion for FRP under arbitrary stress states has been established. Based on results of RVE simulations, a database of stress state and corresponding failure model was created. This database was used to train a simple NN on the posed classification task. It could be shown, that the NN achieves high accuracy on training, testing and validation data. Additionally, a large share of misclassifications is based on very narrow margins. Useable accuracy can therefore be further increased by incorporating engineering judgement. The current version of the model can be used for post hoc analyses of FRP parts, efficiently using the failure information from micro-scale on the meso-scale.

The strong oscillations of loss and accuracy during training could be indicators of a suboptimal network architecture or the demand for additional data. Therefore, generating additional data and focusing the hyperparameter optimization on modulating the architecture are expected to further improve model performance. Additionally, transferring the trained model to a user material routine would further enhance its capabilities and allow the usage during simulations to trigger element deletion.

To further take effects from the heterogeneity in the microstructure observable in mechanical joints of FRP into account, the data generation can directly be extended to statistical volume elements. This allows to capture the influence that local variations in fiber volume content have on failure initiation.

Funding

This research was funded by the Deutsche Forschungsgemeinschaft (DFG, German Research Foundation) – TRR 285/2 – 418701707 – sub-project A03.

References

[1] D. Rajak, D. Pagar, P. Menezes, and E. Linul, “Fiber-Reinforced Polymer Composites: Manufacturing, Properties, and Applications,” Polymers, vol. 11, no. 10. MDPI AG, p. 1667, Oct. 12, 2019. doi: 10.3390/polym11101667.

[2] Prashanth S, Subbaya KM, Nithin K, Sachhidananda S, “Fiber Reinforced Composites - A Review,” Journal of Material Science & Engineering, vol. 06, no. 03. OMICS Publishing Group, 2017. doi: 10.4172/2169-0022.1000341.

[3] Y. Chen, X. Yang, M. Li, K. Wei, and S. Li, “Mechanical behavior and progressive failure analysis of riveted, bonded and hybrid joints with CFRP-aluminum dissimilar materials,” Thin-Walled Structures, vol. 139. Elsevier BV, pp. 271–280, Jun. 2019. doi: 10.1016/j.tws.2019.03.007.

[4] B. Ravichandran and M. Balasubramanian, “Joining methods for Fiber Reinforced Polymer (FRP) composites − A critical review,” Composites Part A: Applied Science and Manufacturing, vol. 186. Elsevier BV, p. 108394, Nov. 2024. doi: 10.1016/j.compositesa.2024.108394.

[5] R. Kupfer, L. Schilling, S. Spitzer, M. Zichner, and M. Gude, “Neutral lightweight engineering: a holistic approach towards sustainability driven engineering,” Discover Sustainability, vol. 3, no. 1. Springer Science and Business Media LLC, May 27, 2022. doi: 10.1007/s43621-022-00084-9.

[6] B. Gröger, J. Gerritzen, A. Hornig and M. Gude, „Developing a numerical modelling strategy for metallic pin pressing processes in fibre reinforced thermoplastics to investigate fibre rearrangement mechanisms during joining“ Proc IMechE Part L: J Materials: Design and Applications (in press)

[7] A. Kaddour and M. Hinton, “Maturity of 3D failure criteria for fibre-reinforced composites: Comparison between theories and experiments: Part B of WWFE-II,” Journal of Composite

Materials, vol. 47, no. 6–7. SAGE Publications, pp. 925–966, Mar. 2013. doi: 10.1177/0021998313478710.

[8] L. Wan, Z. Ullah, D. Yang, and B. G. Falzon, “Comprehensive inter-fibre failure analysis and failure criteria comparison for composite materials using micromechanical modelling under biaxial loading,” Journal of Composite Materials, vol. 57, no. 18. SAGE Publications, pp. 2919–2932, May 31, 2023. doi: 10.1177/00219983231176609.

[9] F. Naya, C. González, C. S. Lopes, S. Van der Veen, and F. Pons, “Computational micromechanics of the transverse and shear behavior of unidirectional fiber reinforced polymers including environmental effects,” Composites Part A: Applied Science and Manufacturing, vol. 92. Elsevier BV, pp. 146–157, Jan. 2017. doi: 10.1016/j.compositesa.2016.06.018.

[10] B. Liang et al., “Multi-scale modeling of mechanical behavior of cured woven textile composites accounting for the influence of yarn angle variation,” Composites Part A: Applied Science and Manufacturing, vol. 124. Elsevier BV, p. 105460, Sep. 2019. doi: 10.1016/j.compositesa.2019.05.028.

[11] D. Pulungan, G. Lubineau, A. Yudhanto, R. Yaldiz, and W. Schijve, “Identifying design parameters controlling damage behaviors of continuous fiber-reinforced thermoplastic composites using micromechanics as a virtual testing tool,” International Journal of Solids and Structures, vol. 117. Elsevier BV, pp. 177–190, Jun. 2017. doi: 10.1016/j.ijsolstr.2017.03.026.

[12] G. Balokas, S. Czichon, and R. Rolfes, “Neural network assisted multiscale analysis for the elastic properties prediction of 3D braided composites under uncertainty,” Composite Structures, vol. 183. Elsevier BV, pp. 550–562, Jan. 2018. doi: 10.1016/j.compstruct.2017.06.037.

[13] J. Chen, L. Wan, Y. Ismail, J. Ye, and D. Yang, “A micromechanics and machine learning coupled approach for failure prediction of unidirectional CFRP composites under triaxial loading: A preliminary study,” Composite Structures, vol. 267. Elsevier BV, p. 113876, Jul. 2021. doi: 10.1016/j.compstruct.2021.113876.

[14] L. Wan, Z. Ullah, D. Yang, and B. G. Falzon, “Probability embedded failure prediction of unidirectional composites under biaxial loadings combining machine learning and micromechanical modelling,” Composite Structures, vol. 312. Elsevier BV, p. 116837, May 2023. doi: 10.1016/j.compstruct.2023.116837.

[15] P. Soden, M. Hinton, A. Kaddour, “Lamina properties, lay-up configurations and loading conditions for a range of fibre-reinforced composite laminates,” Composites Science and Technology, vol. 58, no. 7. Elsevier BV, pp. 1011–1022, Jul. 1998. doi: 10.1016/s0266-3538(98)00078-5.

[17] M. E. Johnson, L. M. Moore, and D. Ylvisaker, “Minimax and maximin distance designs,” Journal of Statistical Planning and Inference, vol. 26, no. 2. Elsevier BV, pp. 131–148, Oct. 1990. doi: 10.1016/0378-3758(90)90122-b.

[18] S. Wessing, “Two-stage methods for multimodal optimization,” Technische Universität Dortmund, 2015, doi: 10.17877/DE290R-7804.

[19] V. R. Joseph, “Space-filling designs for computer experiments: A review,” Quality Engineering, vol. 28, no. 1. Informa UK Limited, pp. 28–35, Jan. 02, 2016. doi: 10.1080/08982112.2015.1100447.

[20] R. G. Cuntze and A. Freund, “The predictive capability of failure mode concept-based strength criteria for multidirectional laminates,” Composites Science and Technology, vol. 64, no. 3–4. Elsevier BV, pp. 343–377, Mar. 2004. doi: 10.1016/s0266-3538(03)00218-5.

[21] Proceedings of the European Conference on Spacecraft Structures, Materials and Mechanical Testing 2005 (ESA SP-581). 10-12 May 2005, Noordwijk, The Netherlands. Edited by Karen Fletcher. Published on CD-Rom, id.138.1

[23] Diez, C., Ballal, N. & "rao014" Open-lasso-python/lasso-python: Home of the open-source CAE Library Lasso-Python. GitHub Repository., https://github.com/open-lasso-python/lasso-python

[24] P. Winkler, N. Koch, A. Hornig, and J. Gerritzen, “OmniOpt – A Tool for Hyperparameter Optimization on HPC,” Lecture Notes in Computer Science. Springer International Publishing, pp. 285–296, 2021. doi: 10.1007/978-3-030-90539-2_19.

[25] P. Ramachandran, B. Zoph, and Q. V. Le, “Searching for Activation Functions,” 2017, arXiv. doi: 10.48550/ARXIV.1710.05941.

[26] D. P. Kingma and J. Ba, “Adam: A Method for Stochastic Optimization,” 2014, arXiv. doi: 10.48550/ARXIV.1412.6980.

[27] L. Yang, Y. Yan, Y. Liu, and Z. Ran, “Microscopic failure mechanisms of fiber-reinforced polymer composites under transverse tension and compression,” Composites Science and Technology, vol. 72, no. 15. Elsevier BV, pp. 1818–1825, Oct. 2012. doi: 10.1016/j.compscitech.2012.08.001.

[16] F. Rickhey, T. Park, and S. Hong, “Damage prediction in thermoplastics under impact loading using a strain rate-dependent GISSMO,” Engineering Failure Analysis, vol. 149. Elsevier BV, p. 107246, Jul. 2023. doi: 10.1016/j.engfailanal.2023.107246.

[22] W. Tian, L. Qi, X. Chao, J. Liang, and M. Fu, “Periodic boundary condition and its numerical implementation algorithm for the evaluation of effective mechanical properties of the composites with complicated micro-structures,” Composites Part B: Engineering, vol. 162. Elsevier BV, pp. 1–10, Apr. 2019. doi: 10.1016/j.compositesb.2018.10.053.